

LOCKHEED MARTIN ENERGY RESEARCH LIBRARIES



3 4456 0515386 5

CENTRAL RESEARCH LIBRARY
DOCUMENT COLLECTION

cy.1

ORNL-4774
UC-33 - Propulsion Systems and
Energy Conversion

ORNL ISOTOPIC POWER FUELS
QUARTERLY REPORT
FOR PERIOD ENDING DECEMBER 31, 1971

Eugene Lamb
R. G. Donnelly

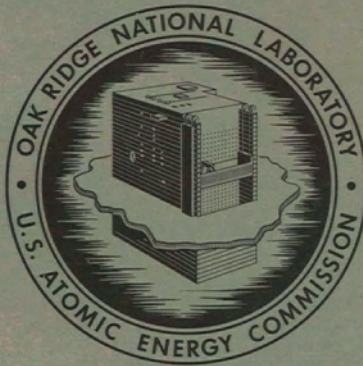
OAK RIDGE NATIONAL LABORATORY
CENTRAL RESEARCH LIBRARY
DOCUMENT COLLECTION

LIBRARY LOAN COPY

DO NOT TRANSFER TO ANOTHER PERSON

If you wish someone else to see this
document, send in name with document
and the library will arrange a loan.

UCN-7969
(3-67)



OAK RIDGE NATIONAL LABORATORY

operated by

UNION CARBIDE CORPORATION

for the

U.S. ATOMIC ENERGY COMMISSION

Printed in the United States of America. Available from
National Technical Information Service
U.S. Department of Commerce
5285 Port Royal Road, Springfield, Virginia 22151
Price: Printed Copy \$3.00; Microfiche \$0.95

This report was prepared as an account of work sponsored by the United States Government. Neither the United States nor the United States Atomic Energy Commission, nor any of their employees, nor any of their contractors, subcontractors, or their employees, makes any warranty, express or implied, or assumes any legal liability or responsibility for the accuracy, completeness or usefulness of any information, apparatus, product or process disclosed, or represents that its use would not infringe privately owned rights.

ORNL-4774

Contract No. W-7405-eng-26

ISOTOPES DEVELOPMENT CENTER

ORNL ISOTOPIC POWER FUELS QUARTERLY REPORT
FOR PERIOD ENDING DECEMBER 31, 1971

Eugene Lamb

Isotopes Division

R. G. Donnelly

Metals and Ceramics Division

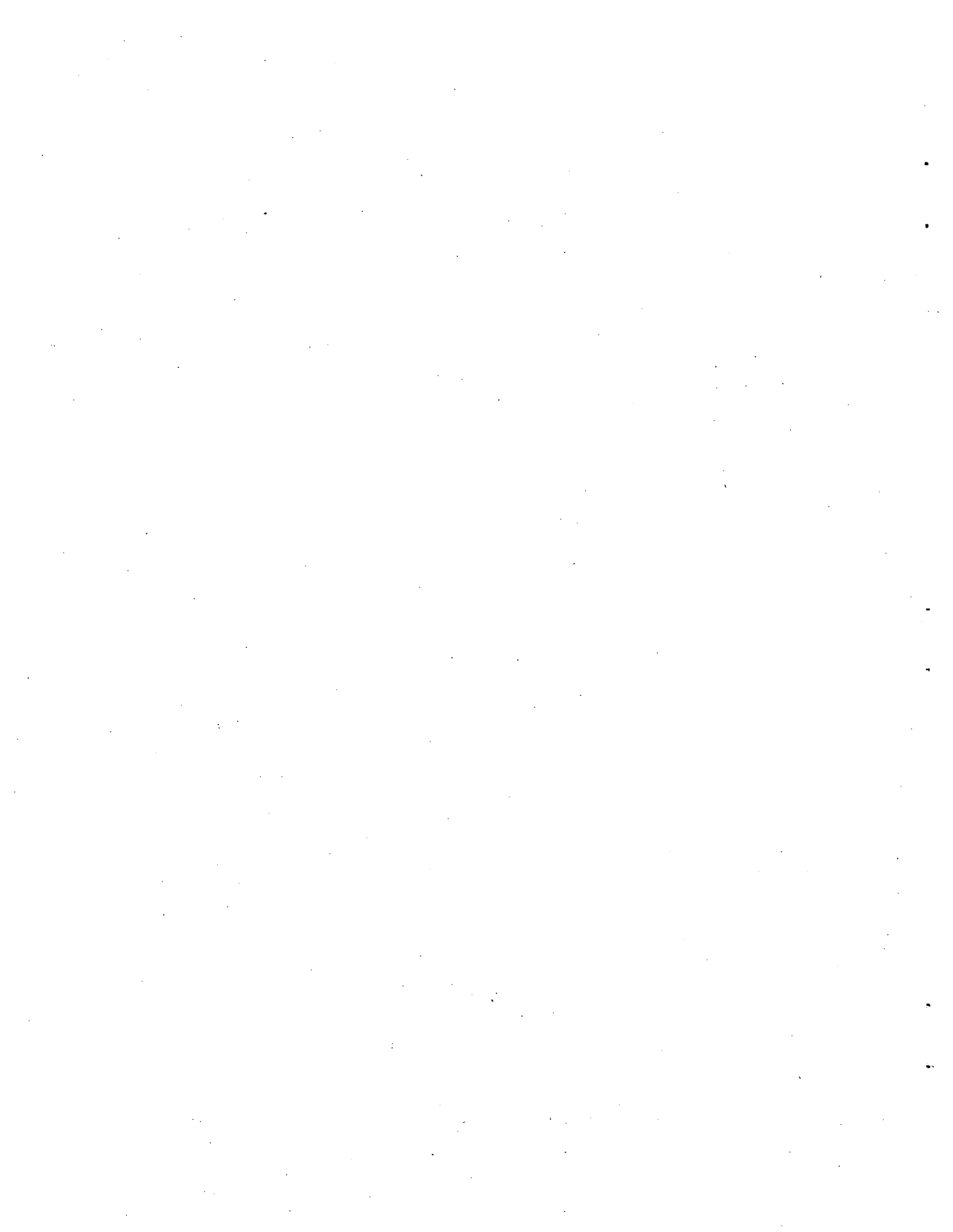
MARCH 1972

OAK RIDGE NATIONAL LABORATORY
Oak Ridge, Tennessee 37830
operated by
UNION CARBIDE CORPORATION
for the
U.S. ATOMIC ENERGY COMMISSION

LOCKHEED MARTIN ENERGY RESEARCH LIBRARIES



3 4456 0515386 5



CONTENTS

	<u>Page</u>
SUMMARY	1
INTRODUCTION	2
CURIUM-244 FUEL DEVELOPMENT	2
Curium-244 Oxide Fuel Development and Properties	2
²⁴⁴ Cm ₂ O ₃ Compatibility	2
Cm ₂ O ₃ Heat Capacity	2
Emissivity of ²⁴⁴ Cm ₂ O ₃	2
Curium-244-Noble Metal Compound Fuel Development and Properties	3
Curium-244 Cermet Fuel Development and Properties	3
Preparation of Sized ²⁴⁴ Cm ₂ O ₃ Particles	4
Curium Source Test	6
Impact Testing of Heat Source Materials	9
PLUTONIA-CURIA PELLETT FABRICATION FOR ²³⁸ PuO ₂ AGING EXPERIMENT	9
Chemical Vapor Deposition Development	10
THULIUM	11
Vapor Pressure of Tm ₂ O ₃ -Yb ₂ O ₃	11
¹⁷⁰ Tm ₂ O ₃ Compatibility	12
CLADDING MATERIALS PROGRAM	12
Preparation of Pt-Rh-W Sheet	12
Development of Improved Alloys	15
Characterization of Iridium	16
PHYSICAL METALLURGY OF REFRACTORY ALLOYS	18
Effect of Oxygen Contamination of the Mechanical Properties of T-111	18
Effect of Oxygen on the Mechanical Properties of 0.090-in.-thick T-111	20
Contamination Studies of T-111 and TZM by Impurities Outgassed from Graphite and Min-K 1301	22
Contamination Studies of T-111 and TZM by Water Vapor	24
Effect of Oxygen Contamination on the Mechanical Properties of Molybdenum-Base Alloys	25
Effect of CO-Gas Contamination on the Mechanical Properties of Molybdenum-Base Alloys	26

	<u>Page</u>
MATERIALS COMPATIBILITY TESTING FOR THE LASL-DART PROJECT	28
REFERENCES	29

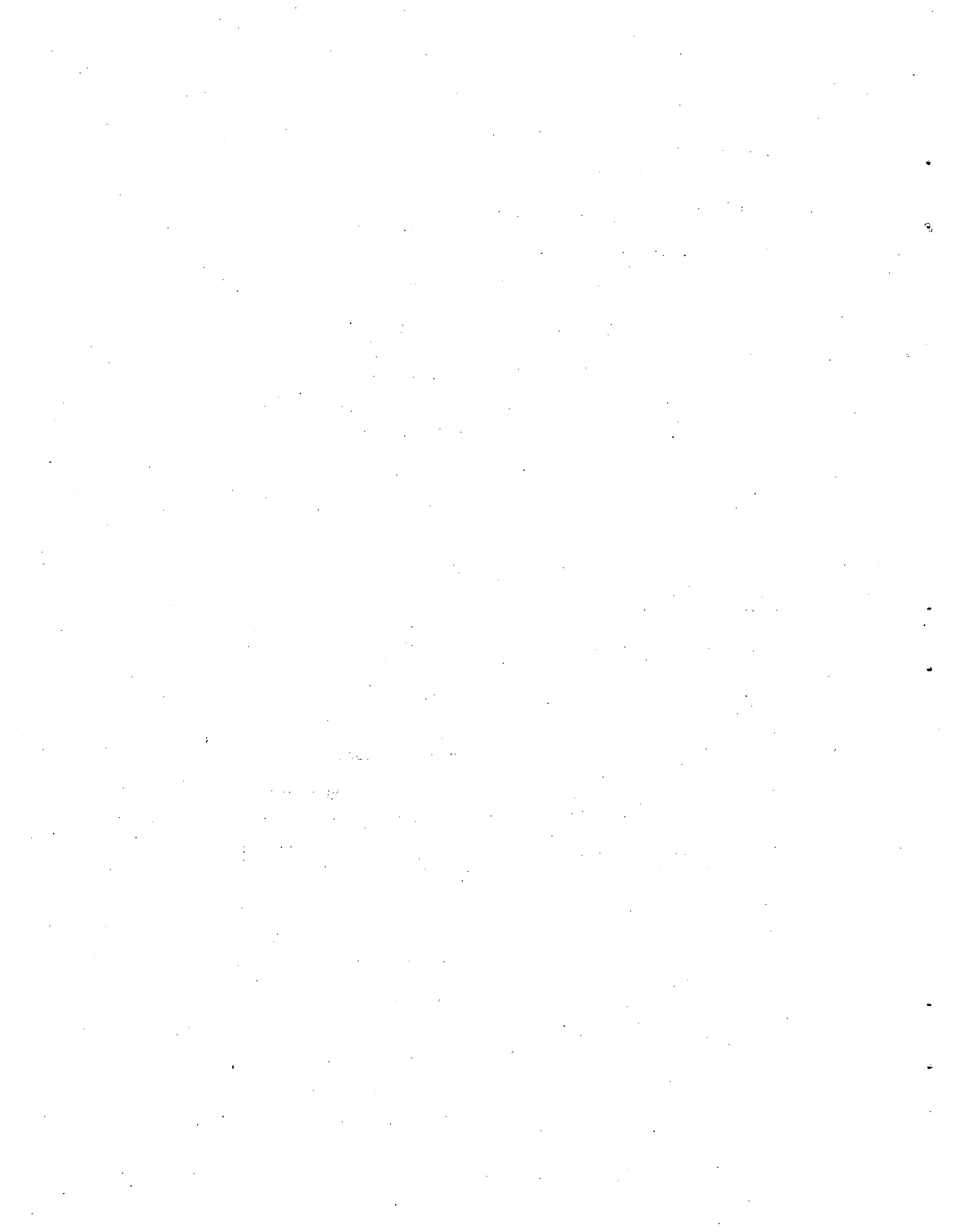
LIST OF TABLES

Table 1. Rates of Effusion, and Partial and Total Pressures of Various Species Above Solid Tm_2O_3 in Small Knudsen Cell at 1900°C	11
Table 2. Current Status of $^{170}Tm_2O_3$ -Refractory Metal Compatibility Program	12
Table 3. Bend Formability Evaluation of Pt-Rh-W Alloys at Room Temperature	13
Table 4. Room- and Elevated-Temperature Tensile Properties of the Platinum-Base Alloys Recrystallized 1 hr at 1200°C	15
Table 5. Effect of 1-hr Annealing Treatment on Hardness, Recrystallization, and Bend Ductility of Unalloyed Iridium Sheet	16
Table 6. Room- and Elevated-Temperature Tensile Properties of Unalloyed Iridium Recrystallized 1 hr at 1500°C	17
Table 7. Tensile Properties of 20-mil Sheet T-111 Specimens As-Doped with Various Levels of Oxygen at 825°C	19
Table 8. Tensile Properties of 40-mil Sheet T-111 Specimens As-Doped with Various Levels of Oxygen at 825°C	19
Table 9. Effect of Oxygen on the Tensile Properties of 90-mil-thick T-111 at 825°C	22
Table 10. Contamination of 0.020-in.-thick Sheet Specimens of T-111 and Molybdenum-Coated T-111 in a Simulated Pioneer Heat Source Environment	23
Table 11. The Effect of Impurities Degassed from Graphite and Min-K 1301 on the Room-Temperature Tensile Properties of 20-mil-thick T-111 and TZM	23
Table 12. Contamination of T-111 Exposed to 1×10^{-5} Torr Water Vapor at 825°C	24
Table 13. Effect of Water Vapor Contamination on the Room-Temperature Tensile Properties of T-111	25

	<u>Page</u>
Table 14. Tensile Properties of 20-mil-thick TZM Exposed to 1×10^{-5} Torr Water Vapor at 825°C	25
Table 15. Tensile Properties of 20-mil-thick TZM and Mo-46% Re Sheet Specimens Contaminated with Oxygen at 825°C	26
Table 16. Effects of Heat Treatment and Testing Temperature on the Tensile Properties of TZM Specimens Doped with Oxygen for 207 hr at 1000°C and 1×10^{-5} Torr Oxygen Pressure	27
Table 17. Tensile Properties of 20-mil-thick TZM and Mo-46% Re Sheet Specimens Contaminated with CO Gas at 825°C and 1×10^{-5} Torr Oxygen Pressure	27
Table 18. Visual Observations from Compatibility Tests of of Graphite with Several Materials for 500 hr at 1300, 1400, and 1500°C	28
Table 19. Conditions for 500-hr Metal Capsule Compatibility Tests	29

LIST OF FIGURES

Fig. 1. Apparatus for Emissivity Experiment	3
Fig. 2. ^{244}Cm Source Test Capsule After Removal from Vacuum Chamber	7
Fig. 3. ^{244}Cm Source Test Capsule After Opening	7
Fig. 4. One-Pound Ingots of Pt-Rh-W Alloys Produced by Electron-Beam Melting and Drop-Casting	14
Fig. 5. Forty-Mil Sheet Produced by Hot-Rolling Pt-Rh-W Drop-Cast Ingots in Air at 1200-1300°C	14
Fig. 6. Room-Temperature Ductility of T-111 Specimens as a Function of the Amount of Oxygen Doped at 825 and 1000°C	20
Fig. 7. Elevated-Temperature Ductility of T-111 Specimens as a Function of the Amount of Oxygen Doped at 825 and 1000°C	20
Fig. 8. Surface and Edge Cracking Behavior of T-111 Tensile Specimens Doped with Approximately 300 ppm Oxygen as a Function of Test Temperature	21



ORNL ISOTOPIC POWER FUELS QUARTERLY REPORT
FOR PERIOD ENDING DECEMBER 31, 1971

Eugene Lamb and R. G. Donnelly

SUMMARY

The emissivity of $^{244}\text{Cm}_2\text{O}_3$ is being determined as a function of the wavelength and temperature. A high-temperature vacuum furnace with TGA and DTA units has been fabricated that will enable the kinetics of the reaction between Cm_2O_3 and the platinum-like metals to temperatures near 2000°C to be studied. Work continues on the preparation of microparticles for cermet development using loaded ion-exchange beads. Gadolinium is being used as a stand-in for curium in the development phase. Good-quality particles have been produced with Rexyn 102H and IRC-72 resins. The curium source test was disassembled after 644 days of operation at 1000 to 1200°C. The primary vacuum chamber was opened, and the capsule was removed and opened.

ORNL hot-pressed the required number of fuel pellets for the $^{238}\text{PuO}_2$ Aging Experiment and shipped them to Donald W. Douglas Laboratories.

The apparent vapor pressure of Tm_2O_3 at 1900°C using small and large Knudsen cells is 1.90×10^{-7} and 1.03×10^{-7} atm, respectively.

One-pound ingots of three Pt-Rh-W alloys have been fabricated into sheet by hot-rolling electron-beam-melted ingots. Of the three, the Pt-26% Rh-8% W alloy appears to be the most fabricable. Additional Pt-Rh-W alloys with small additions of hafnium and titanium have also been fabricated into sheet. In general, these alloys exhibit superior mechanical properties, particularly at elevated temperatures. The physical and mechanical properties of unalloyed iridium have been determined as a first step in an attempt to resolve problems of ductility and fabricability.

The sensitivity of T-111 and molybdenum alloys to contaminants such as oxygen, water vapor, and other gases which are present in Pioneer radioisotope thermal generators has been determined. In general, the molybdenum alloys appear far less sensitive to these impurities than T-111.

Nonfuel materials compatibility tests in support of the DART Program at Los Alamos have been completed and partially evaluated. Preliminary results indicate that tungsten interacts the least with graphite under the test conditions.

INTRODUCTION

The development of fuel forms with optimum design for use at temperatures up to 2000°C involves obtaining the characteristics of isotopic power and heat sources for anticipated applications in aerospace, terrestrial, and marine environments. The physical and chemical properties of the compound and source form, such as thermal conductivity, density, gas retention, and melting point, must be determined. Compatibility of the fuel form with container materials must be established to ensure adequate containment during the intended lifetime of the mission.

CURIUM-244 FUEL DEVELOPMENT

(Division of Space Nuclear Systems Program 04 30 05 03)

Curium-244 Oxide Fuel Development and Properties

 $^{244}\text{Cm}_2\text{O}_3$ Compatibility

The report entitled *Compatibility of Curium Oxide with Refractory Metals at 1650°C and 1850°C* is being reproduced.

 Cm_2O_3 Heat Capacity

The complete calorimeter system has been operated satisfactorily, and the unit has been tested to 1400°C. The new elevator mechanism is operating very satisfactorily.

The cell backplate containing the viewing window, glove ports, etc. has been installed on the cell containing the Cm_2O_3 heat capacity apparatus. Several minor alterations were made to the cell atmosphere control system. Leak checking and operation of the cell under inert atmosphere conditions are continuing.

Emissivity of $^{244}\text{Cm}_2\text{O}_3$

The objective of the experiment is to determine the emissivity (ϵ) of $^{244}\text{Cm}_2\text{O}_3$ as a function of the wavelength and temperature. The wavelength (λ) region of interest would be from the visible to at least 17 μ . The total emissivity would be obtained by averaging the ϵ vs λ curves.

A block diagram of the experimental setup is shown in Fig. 1. Fuel would be located in the furnace, and reflected light from extraneous sources would be kept to a minimum. The sample would be fabricated so that it would contain a blackbody hole.

The mode of operation would be the following: light from two sources on the pellet (surface and blackbody hole) would be collimated into two beams. These beams would be chopped at different frequencies, sent through a monochromator, and detected. The two beams of different chopping frequencies would be recovered from the detector by using AC amplifiers

called lock-in amplifiers. During this process, the monochromator would be scanning over a range of wavelengths. The two chopping frequencies would be high enough such that the two recovered signals are representative of essentially the same wavelength. The two light beams impinge on the same detector and are summed by the detector. The lock-in amplifiers are able to recover the original values used to obtain that sum. We have tested this recovery method and found that it works very well. Both phototubes and infrared-sensitive thermistors will be used as detectors in the experiment. The study of the overall instruments needed has been made, and specific instruments have been chosen. The experimental method is sound, and the system can be operated in many different ways to obtain the same emissivity results, enabling us to check the methods and thus obtain data that are more reliable.

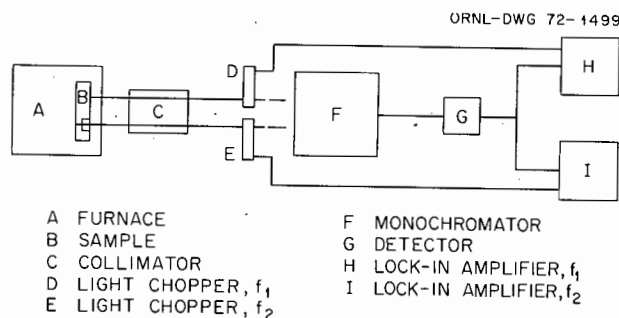


Fig. 1. Apparatus for Emissivity Experiment.

Curium-244-Noble Metal Compound Fuel Development and Properties

A high-temperature vacuum furnace with TGA and DTA units has been fabricated. This furnace will enable us to study the kinetics of the reaction between Cm_2O_3 and the platinum-like metals to temperatures near 2000°C . Melting point determinations, as well as helium release experiments, can be performed with the unit. The furnace is being installed in the glove box.

Curium-244 Cermet Fuel Development and Properties

This task involves the preparation of sized $^{244}\text{Cm}_2\text{O}_3$ particles for use in cermets and the determination of ranges of fabrication parameters for Mo- ThO_2 as a stand-in for Mo- $^{244}\text{Cm}_2\text{O}_3$ and noble metal- $^{244}\text{Cm}_2\text{O}_3$ cermets. The preparation of cermets requires sized particles of Cm_2O_3 which are incorporated into the metal matrix to form the composite fuel. Of the several methods available to produce sized particles, the ion-exchange procedure offers the potential advantages of efficient utilization of ^{244}Cm without recycle, adaptability to manipulator cell operation, and simplicity of procedure.

Our aim is to develop cermet fuel forms with the most desirable combination of properties and to reduce the in-cell development requiring curium. We are specifically attempting to structure the cermet to provide for helium release.

Preparation of Sized $^{244}\text{Cm}_2\text{O}_3$ Particles

Gadolinium is being used as a stand-in for curium in the development of a process for the manufacture of microparticles. The essential steps in the process are as follows: (1) an ion-exchange resin is loaded with gadolinium; (2) the organic material is decomposed in an inert atmosphere; (3) the carbon is removed by oxidation; and (4) the particles are sintered.

Good-quality Gd_2O_3 particles have been produced using the ion-exchange resins Rexyn 102H and IRC-72. These particles have a bulk density of 5.0-5.2 g/cm^3 , which corresponds to a packing efficiency of 60.2-62.5% based on a theoretical density of 8.31 g/cm^3 for Gd_2O_3 as calculated from x-ray diffraction data. The packing efficiencies are in the range expected of materials of this type so that the particle density is apparently nearly 100% of theoretical.

The average particle diameter of the Gd_2O_3 beads produced from Rexyn 102H and IRC-72 was determined. Measurements were made of the diameters of a large number of particles as shown in microphotographs. In the case of the nonspherical beads from Rexyn 102H, the diameters were measured in the horizontal direction, then in the vertical direction as they fell on the photograph. Random orientation was assumed.

The beads produced using IRC-72 had an average diameter of 219 microns. The standard deviation was 55 microns. The largest particle diameter was 342 microns, and the smallest was 122 microns. It was observed that smaller particles had existed but fused together to form agglomerates. These values are based on 25 measurements.

Measurements of samples from two different batches of beads produced using Rexyn 102H gave average diameters of 258 microns and 259 microns. The numbers of measurements were 25 and 18 and the standard deviations were 58 and 44 microns, respectively. The largest diameter observed in either batch was 362 microns; the smallest was 187 microns.

The oxide bead size is controlled by the size of the original resin beads when other conditions are uniform. Thus, a narrower particle-size range could be obtained by closer sizing of the original resin. The fines had been washed from the resin used to produce the measured beads. No other sizing had been carried out.

Experience has shown that high-density beads can be obtained only from resin beads that are essentially 100% loaded with gadolinium. Furthermore, the time which can be allowed for loading will be limited by radiation damage of the organic ion-exchange beads when curium is used. An allowable time of 4-5 hr has been estimated. A rapid loading procedure is required and varying procedures have been tested.

Preliminary results indicate that one of the methods tested meets the requirements of the process. More than 99% of theoretical loading was achieved in 4 hr. In this process the resin in the NH_4^+ form is contacted with three successive portions of $\text{Gd}(\text{NO}_3)_3$ solution. Boiling and agitation

are continued throughout the process. A second test of the method using GdCl_3 solution instead of $\text{Gd}(\text{NO}_3)_3$ has been carried out, but analytical results are not yet complete.

Another type of loading process was investigated. The resin in the hydrogen form is heated in GdCl_3 solution along with Gd_2O_3 . The Gd^{3+} ion reacts with the resin releasing H^+ ion. The H^+ reacts with the oxide to produce more Gd^{3+} ion and water. Thus, the GdCl_3 acts as a carrier and is not consumed.

Previous observations indicated that the rate of loading was controlled by the rate of diffusion into the beads. When the loaded resin was separated into large and small particle size fractions, the smaller particles showed heavier loading. Furthermore, the oxide beads produced from partially loaded resin were often hollow. This effect indicated that the interior had contained little gadolinium.

It was reasoned that the rate of diffusion of Gd^{3+} into the beads would be proportional to the concentration of Gd^{3+} in the solution. Consequently, the process was carried out using 6 *N* GdCl_3 rather than the 2-3 *N* concentrations used in previous tests. In 4 hr 92% loading was achieved. This loading is better than that previously achieved in 4 hr by the oxide slurry method, but the rate is inferior to that of the ammonium-form resin method and is marginal for our process.

The oxide loading process would have advantages when applied to a large-scale production process if a longer reaction time were allowable or if an ion showing faster reaction kinetics were involved. A single bath could be used for many batches of resin. Makeup oxide would be added as required.

Good-quality particles have been produced in several experimental runs using the ion-exchange resins Rexyn-102H and IRC-72, which are of the carboxylic or weak acid type. In some runs, the beads shattered into fragments during the decomposition, oxidation, or sintering steps. (These operations are carried out consecutively in the same container without opportunity for observation.) An investigation of the cause of the observed bead fracturing was made using a hot-stage microscope. With this microscope the sample can be observed and photographed in a controlled atmosphere while it is being heated to temperatures up to 1300°C.

The beads were found to shatter late in the decomposition or carbonization step when the argon contained appreciable air. When a pure argon atmosphere was used, shattering did not occur.

Other photographs were made which confirm the tendency of oxygen in the argon to cause shattering of the beads. Both IRC-72 and Rexyn-102H were investigated with similar results.

The fluidized bed tube in which the laboratory production runs had been made was examined and found to contain cracks through which air could enter. A successful run was made after sealing the cracks.

An apparatus is being constructed for the experimental production of $^{244}\text{Cm}_2\text{O}_3$ beads.

Curium Source Test

Disassembly of the curium source test was accomplished on December 15-17, 1971. The primary vacuum chamber was opened, and the capsule was removed and opened. The source, originally built in February 1970, operated continuously in its insulated chamber at temperatures from 1000 to 1200°C through February 1971 and 1100 to 1200°C since.¹ The source initially contained 956 W(th) of ^{244}Cm as the sesquioxide with a power density of 2.32 W(th)/g. This material has subsequently decayed to 890 W(th) and a power density of 2.16 W(th)/g.

Examination of the vent line was inconclusive in determining where a leak in the helium venting system occurred during the test period. Removal of the top of the capsule revealed a granular material adhering to the top of the main capsule body above the pellets and nearly filling the 1/4-in.-thick space between the top of the pellets and bottom of the vent disk. Calorimetry of this material shows that it was mostly curium, indicating that migration of some of the curium had taken place.

The curium pellets could not be removed from the capsule by use of probing and chipping tools. The capsule and pellets were sealed in a Hastelloy C capsule containing argon. Details of the opening sequence are presented below.

Helium was admitted to the vacuum chamber to decrease the capsule temperature from 1090°C to 900°C when the helium pressure reached ≈ 1 atmosphere. The oxygen level in the cell was reduced to 2,500 ppm by flowing argon. The vacuum chamber was opened by grinding off the weld and lifting the lid. An inspection of the insulation and vent tube assembly revealed no apparent cracks or severe oxidation.

The inner insulation cap was bonded to the top of the inner support cylinder of tungsten multifoil insulation, but was broken free and removed. Visual inspection of the capsule showed no oxidation of its upper portion. All thermocouple wires were cut, and the six socket-head cap screws holding the capsule to the baseplate were removed. The vent tube was then crushed, the capsule handling tool was attached to the capsule, and the capsule was removed from the insulation. At this time the oxygen level in the cell atmosphere was 4,000 ppm. Visual inspection of the capsule revealed no flaws or cracks. Inspection of the vent tube assembly was inconclusive as to where the leak had developed in the vent system. The capsule was transferred to an adjacent cell and stored overnight in an argon atmosphere with a maximum oxygen level of 1,000 ppm.

Photographs taken of the capsule the following day are shown in Figs. 2 and 3. Figure 2 shows surface oxidation of the capsule, most of which is believed to have occurred during exposure to the cell atmosphere. During the second day the top of the capsule was removed by using a bonded diamond rotary cut-off saw. Figure 3 shows the capsule with the pellets exposed (upper portion in the picture) and the bottom view of the vent disk (lower portion of picture). As shown in Fig. 3, each of the seven pellet holes appears to have a column of granulated substance reaching from the pellet holes to the bottom of the vent disk. The granulated substance was scraped from the bottom of the vent disk and from the top of the pellet holes and stored in identified containers. When the top portion of the capsule was moved to a position to scrape off the granulated substance, some black powder poured out of the slot in the vent disk. This material was placed in an identified container. Once the granulated material had been cleaned from the pellet holes, the tops of the pellets appeared to be sharp and flat.

Thin wisps of smoke were observed coming from the top of the pellets. At this time the oxygen level in the cell was 1,400 ppm. Closer observation revealed that smoke was coming from each of the seven holes. A stainless steel scoop was held $\sim 1/2$ in. above the pellet holes to determine if the smoke would condense on the bottom of the scoop, but no condensation on the scoop was observed. We were unable to determine the exact origin of the smoke (fuel or capsule wall), but we believe the most reasonable explanation to be oxidation of the tungsten and generation of fine tungsten oxide particles.



Fig. 2. ^{244}Cm Source Test Capsule After Removal from Vacuum Chamber.

An attempt to dump the pellets failed because they were lodged tight. The pellets could not be broken up with a screw driver. Chipping the pellets from the capsule was considered too slow (~ 6 g in 20 min), and it was decided that the curium could not be



Fig. 3. ^{244}Cm Source Test Capsule After Opening.

recovered in a reasonable time. During chipping of the pellets more smoke was emitted from the hole in the tungsten capsule. The capsule was left overnight under an argon atmosphere containing 650 ppm oxygen.

On the third day the bottom portion of the capsule containing the fuel pellets was placed in a thick-walled Hastelloy C container and seal welded for storage. The top portion of the capsule was placed in a separate stainless steel container with a threaded cap for storage. Calorimeter measurements were made on the heat output of all the powder that was recovered from the capsule. Results of the calorimeter runs are tabulated below.

<u>Description of Material</u>	<u>Weight (g)</u>	<u>Power Density [W(th)/g]</u>
Scrapings from top of pellets	15.85	1.76
Scrapings from bottom of vent disk	29.35	1.70
Powder from inside vent disk	2.50	1.20
Material chipped from pellets	6.55	1.83
Vent tube ^a	<0.25	-
Top of capsule and vent disk ^b	<2.0	-

^aEntire vent tube placed in calorimeter.

^bCapsule and vent disk placed in calorimeter after powder was removed.

The $^{244}\text{Cm}_2\text{O}_3$ pellets had an average power density of 2.32 W/g at the beginning of the experiment. Accounting for 1 year and 10 months decay, the average power density would be 2.16 W/g.

Samples of material taken from different sections of the fuel capsule, as listed in the above calorimetry information, will be analyzed by spark source mass spectrometry. One sample of the $^{244}\text{Cm}_2\text{O}_3$ fuel will be examined by x-ray diffraction, and another sample will be photomicrographed. Another sample of the $^{244}\text{Cm}_2\text{O}_3$ pellet fuel will be used to determine the helium inventory remaining in the fuel.

From the data shown in the above paragraph, 37.6 g of Cm_2O_3 was transported by some mechanism from the holes in the source capsule containing the Cm_2O_3 pellets. Calculations were made to determine if this quantity transported is consistent with the vaporization information available.

Based on measurements of the source capsule temperature during the early part of the experiment, the surface temperature of the Cm_2O_3 pellets from which evaporation could occur was calculated to be 1410°C. The observed transport of material was $\approx 8.4 \times 10^{-8}$ g/cm²·sec based on the total area of the seven holes containing the pellets and based on the transport occurring in vacuum. This transport rate would correspond to a temperature range of 1525 to 1600°C.

The inconsistency between the calculated pellet temperature and the temperature at which the observed vaporization rate should occur leads to the following observations:

1. The actual pellet temperature could have been higher than that calculated.
2. The area of the pellets from which vaporization occurred may have been larger than the superficial area of the top pellet surface, as used in the above calculation of observed transport rate.
3. The transport of Cm_2O_3 in vacuum might be higher than existing data indicate.

The distribution of ^{244}Cm as determined by calorimetric measurements shows that the vent disk functioned properly in retaining the curium within the capsule. Further sectioning of the capsule to determine effects on the fuel and capsule material will be done in FY 1973.

Impact Testing of Heat Source Materials

The gas-powered impact testing gun built by Process Equipment Company was inspected at their plant. Four test shots were made with the following results:

<u>Missile Weight</u> (lb)	<u>Time^a</u> (sec)	<u>Firing Pressure</u> (psi)	<u>Velocity</u> (ft/sec)
2	0.00399	180	250.6
2	0.00401	180	249.4
2	0.00404	180	247.5
1 lb 3-1/2 oz	0.00310	180	322.6

^aTime interval measured across a 1-ft span.

PLUTONIA-CURIA PELLET FABRICATION FOR $^{238}\text{PuO}_2$ AGING EXPERIMENT

(Division of Space Nuclear Systems Program 04 30 05 01 1)

The objective of this experiment is to simulate the effects of ~2-1/2 years of aging in ^{238}Pu space fuels in six months. Oak Ridge National Laboratory Isotopes Division is charged with the task of fabricating the fuel pellets to be used in the experiment. Savannah River Laboratory is responsible for supplying ORNL with $^{238}\text{PuO}_2$ and a ^{242}Cm - $^{238}\text{PuO}_2$ mixture. ORNL hot-pressed the required number of pellets and shipped them to Donald W. Douglas Laboratories, Richland, Washington, in October.

Chemical Vapor Deposition Development

Plutonium-238 oxide was processed to obtain particles in the correct size range and to coat with molybdenum. After chemical processing and screening, 14.09 g of $^{238}\text{PuO}_2$ in the size range of 105-250 μm was recovered. Two 5-g batches of the particles were coated with molybdenum. The resulting molybdenum content of the two runs as determined by weighing was 20.88 and 15.2%. The remaining 4.09 g of $^{238}\text{PuO}_2$ was coated with molybdenum; 13.5 wt % molybdenum was deposited on the particles. The three batches of coated particles were mixed with 1.5 g of coated particles remaining from the three original runs which gave a total coated weight of 18.38 g. The resulting mixture of coated particles had an average molybdenum content of 16.7% as determined by weight. The 18.38 g of molybdenum-coated $^{238}\text{PuO}_2$ particles was hot-pressed in a carbon die lined with 10 mils of Grafoil and 1 mil of tantalum foil. The resulting hot-pressed pellet was placed in a drill press, and seven pellets were core-drilled from the large hot-pressed pellet. After the pellets were core-drilled, approximately 15 mils was ground from each end of the pellets.

The results of the molybdenum-coated pellet fabrications are listed below:

<u>Pellet No.</u>	<u>Height (in.)</u>	<u>Diameter (in.)</u>	<u>Weight (g)</u>	<u>Density (g/cm³)</u>
1	0.200	0.183	0.884	10.24
2	0.192	0.184	0.896	10.23
3	0.202	0.183	0.898	10.30
4	0.199	0.184	0.871	10.04
5	0.203	0.186	0.900	9.95
6	0.201	0.186	0.889	9.92
7	0.202	0.182	0.789	9.20

Pellet 6 had a shallow groove along one side due to core-drill misalignment, and pellet 7 which adjoined pellet 6 in the disk had a deep groove. All seven pellets were wrapped in tantalum foil and placed in a shipping capsule liner.

Five $^{238}\text{PuO}_2$ pellets (PPO) were also fabricated by cold-pressing and sintering. The five pellets were sintered at a temperature of 1625°C for 2 hr. The results of this operation are listed below:

<u>Pellet No.</u>	<u>Height (in.)</u>	<u>Diameter (in.)</u>	<u>Weight (g)</u>	<u>Density (g/cm³)</u>
1	0.206	0.192	0.946	9.68
2	0.228	0.192	1.073	9.92
3	0.219	0.192	1.016	9.77
4	0.231	0.192	0.973	8.87
5	0.174	0.192	0.679	8.22

Pellet 5 had a large chip in one end. All five pellets were wrapped in tantalum foil and placed in a shipping capsule liner. Both shipping capsule liners were welded into shipping capsules. The capsules were placed in a 6-M shipping drum and shipped by air freight to Donald W. Douglas Laboratories on October 26, 1971.

THULIUM

(Division of Isotopes Development Program 08 01 01)

Vapor Pressure of Tm_2O_3 - Yb_2O_3

Experiments to determine the vapor pressure of Tm_2O_3 at $1900^\circ C$ using the small Knudsen cell have been concluded. The apparent vapor pressure of Tm_2O_3 at $1900^\circ C$ calculated from the experimental data is 1.90×10^{-7} atm as shown in Table 1. This value is considerably higher than that based on the data from the large Knudsen cell (1.03×10^{-7} atm). Experiments were performed to determine whether the rate of weight change of the empty Knudsen cell would show a drift after an extended time of use. The result with the large Knudsen cell appeared to indicate that the average rate did not change appreciably after more than two months of continuous use.

Work to correct the water leakage problem inside the vacuum furnace is still in progress. Since attempts to repair the cooling coils at ORNL were unsuccessful, the coils have been returned to the manufacturer for repair. The experiment will be resumed as soon as the repair work is completed.

Table 1. Rates of Effusion, and Partial and Total Pressures of Various Vapor Species Above Solid Tm_2O_3 in Small Knudsen Cell at $1900^\circ C$

Vapor Species	Rate of Effusion ^a (g/cm ² .min) $\times 10^5$	Partial Pressure ^b (atm) $\times 10^7$
TmO	6.33	0.83
Tm	4.73	0.65
O	<u>0.95</u>	<u>0.42</u>
Total	12.01	1.90 ^c

^aCorrected for the weight change of the empty Knudsen cell as well as for the thermal expansion of the orifice.

^bCorrected for the Clausing factor (a transmission probability).

^c"Total" vapor pressure of Tm_2O_3 .

$^{170}\text{Tm}_2\text{O}_3$ Compatibility

Preparation for metallography is near completion for six $^{170}\text{Tm}_2\text{O}_3$ -refractory metal couples exposed at 1600°C for 5,000 hr (Samples S-4, -5, and -8, and A-2, -4, and -9, Table 2). The 500-hr exposure run at 2000°C for the two couples (S-9 and A-5, Table 2) has recently been completed. These couples have been transferred to the High Radiation Level Examination Laboratory (HRLEL) for examination, and preparation for metallic examination is near completion.

Table 2. Current Status of $^{170}\text{Tm}_2\text{O}_3$ -Refractory Metal^a Compatibility Program

Sample No.	Process for Fuel Material Preparation	Exposure Conditions		Status
		Temp (°C)	Time (hr)	
S-1, -2, -6, -7	Sanders Nuclear proprietary process	1600	2500	Exposure completed; examination may be made during FY 1972
S-3, ^b -5, -4, -8	Sanders Nuclear proprietary process	1600	5000	Exposure completed; preparation for metallography in progress for S-4, -5, and -8 (TZM, T-111, and W)
A-1, -3, -6, -8	Savannah River Laboratory process	1600	2500	Exposure completed; examination may be made during FY 1972
A-2, -4, -7, ^b -9	Savannah River Laboratory process	1600	5000	Exposure completed; preparation for metallography in progress for A-2, -4, and -9 (TZM, W, and T-111)
S-9 ^b	Sanders Nuclear proprietary process	2000	500	Exposure completed; preparation for metallography in progress
A-5 ^b	Savannah River Laboratory process	2000	500	Exposure completed; preparation for metallography in progress

^aInner capsule and test disk material: TZM, Ta-10% W, T-111, and W.

^bInner capsule and test disk material for S-3 and A-7 are made of Ta-10% W while those for S-9 and A-5 are made of tungsten.

CLADDING MATERIALS PROGRAM

(Division of Space Nuclear Systems Program 04 30 05 04)

R. G. Donnelly
Metals and Ceramics Division

Preparation of Pt-Rh-W Sheet

To compare the fabricability of the Pt-Rh-W alloy with small changes in composition, 500-g melts of each of three alloys with nominal compositions of Pt-26% Rh-8% W, Pt-30% Rh-10% W, and Pt-30% Rh-10% W-1% Hf-0.1% Ti were electron-beam melted and drop-cast to make 0.5-in.-thick by

1-in.-wide by 2-in.-long ingots as shown in Fig. 4. These ingots were hot-rolled at 1200 to 1300°C without environmental protection to make 0.040-in.-thick sheet (Fig. 5). The hot-rolled sheet was cold-rolled with intermediate anneals to 0.030-in. thickness. Formability of the alloys was then evaluated from standard bend tests carried out in accordance with Materials Advisory Board recommendations (MAB-176-M). Each alloy was heat-treated in vacuum at the appropriate temperature to produce specimens representative of stress-relieved, nominally 50% recrystallized, and fully recrystallized structures. Data from the bend tests are given in Table 3. The alloys were compared at a 4T bend radius followed by other smaller bend radii that provided the basis for calculation of minimum bend radius.

The bend data from the Pt-30% Rh-10% W alloy does not appear to agree with comparable tensile results shown in Table 4. Examination of the test specimens by metallographic procedures indicates probable surface contamination that could affect the ductility of the alloys. We are presently attempting to identify and eliminate this problem in the Pt-2608 alloy.

Table 3. Bend Formability Evaluation of Pt-Rh-W Alloys at Room Temperature

Heat Treatment Temp (°C)	Condi- tion ^a	Bend Radius (T)	Bend Angle	Elon- gation (%)	Bend Strength ^b (psi)
<u>Pt-26% Rh-8% W</u>					
950	SR	4	<40	—	258,000
1000	RC ~50%	4	>90	—	238,000
1100	RC	4	>90	—	156,000
1200	RC	2.7 ^c	90	15.5	144,000
<u>Pt-30% Rh-10% W</u>					
950	SR	4	<30	—	210,000
1000	RC ~50%	4	<20	—	215,000
1100	RC	4	<40	—	200,000
1200	RC	9.2 ^c	90	5.2	117,000
<u>Pt-30% Rh-10% W-1% Hf-0.1% Ti</u>					
950	SR	4	<15	—	351,000
1050	RC ~50%	4	<15	—	344,000
1200	RC	4	<25	—	226,000
1300	RC	9.3 ^c	90	5.1	206,000

^aSR = stress relieved, RC = recrystallized.

^bOuter fiber.

^cCalculated minimum bend radius.

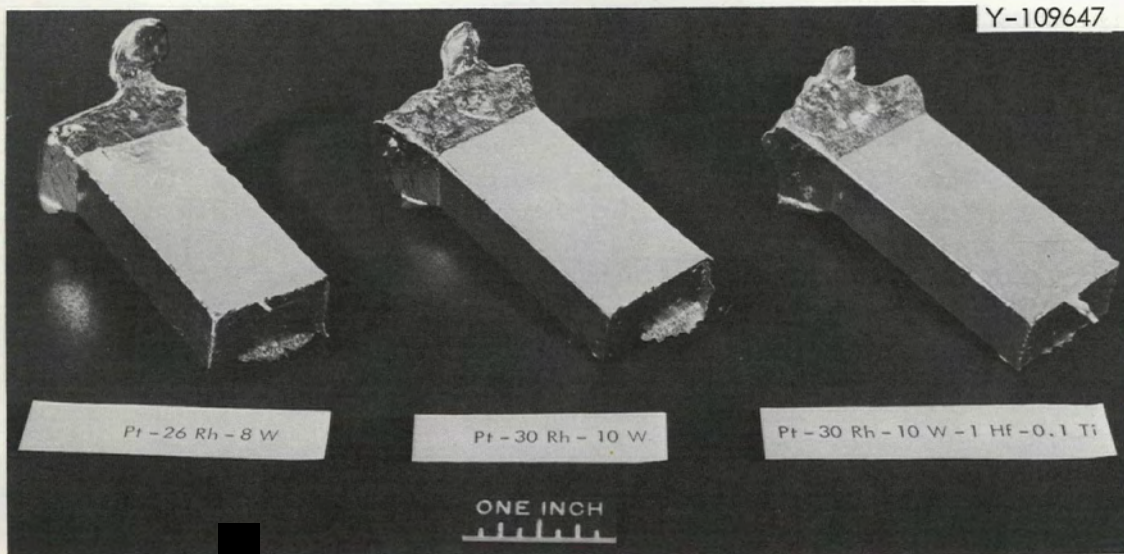


Fig. 4. One-Pound Ingots of Pt-Rh-W Alloys Produced by Electron-Beam Melting and Drop-Casting.

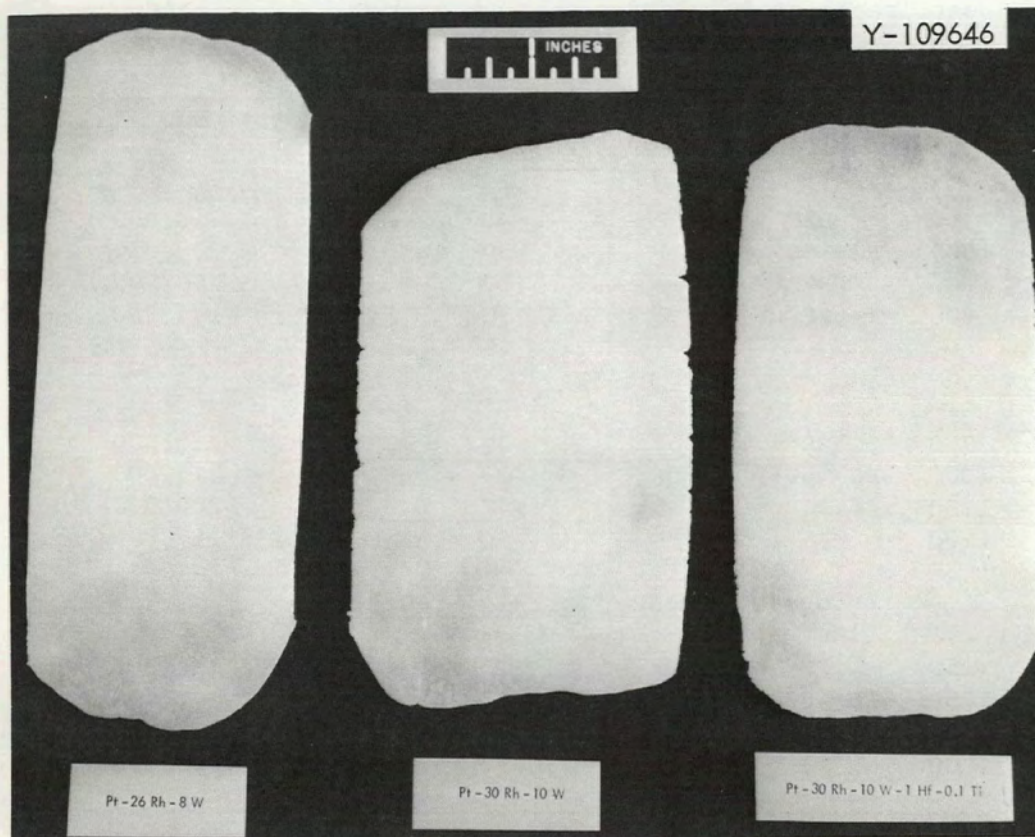


Fig. 5. Forty-Mil Sheet Produced by Hot-Rolling Pt-Rh-W Drop-Cast Ingots in Air at 1200-1300°C.

Development of Improved Alloys

We found that the Pt-30% Rh-12% W alloy cannot be fabricated satisfactorily in temperatures up to 1100°C. The upper limit of tungsten content in the Pt-Rh-W alloy for fabricability, therefore, appears to be between 10-12%.

In order to show the effects of hafnium and titanium on the physical and mechanical properties of the Pt-Rh-W alloy base, four ingots with compositions Pt-30% Rh-8% W-1% Hf-0.2% Ti, Pt-30% Rh-8% W-0.5% Hf-0.2% Ti, Pt-30% Rh-8% W-0.25% Hf-0.1% Ti, and Pt-30% Rh-6% W-0.5% Hf-0.2% Ti were prepared by either electron-beam drop-casting or casting into pancake form. The ingots were first hot-rolled in air in the 1000 to 1230°C range. When the as-cast structure was broken, the alloys were successfully rolled at room temperature to 20- to 35-mil sheet with intermediate anneals between 950 and 1000°C.

Tensile specimens were stamped from the sheet stocks and tested at room and elevated temperatures. Table 4 shows the tensile properties of stabilized alloys together with the data for Pt-Rh-W alloys reported

Table 4. Room- and Elevated-Temperature Tensile Properties of the Platinum-Base Alloys Recrystallized 1 Hr at 1200°C

Alloy Composition (wt %)	Ultimate Tensile Strength (psi)	Elongation (%)
<u>Room Temperature</u>		
Pt-30 Rh	a	a
Pt-30 Rh-6 W	112,000	26
Pt-26 Rh-8 W	a	a
Pt-30 Rh-10 W	118,000	14.5
Pt-30 Rh-6 W-0.5 Hf-0.2 Ti	113,000	19.3
Pt-30 Rh-8 W-0.5 Hf-0.2 Ti	135,000	19.0
Pt-30 Rh-8 W-1 Hf-0.2 Ti	130,000	11.7
<u>760°C (1400°F)</u>		
Pt-30 Rh	48,000	28.8
Pt-30 Rh-6 W	80,000	23.3
Pt-26 Rh-8 W	a	a
Pt-30 Rh-10 W	95,000	28
Pt-30 Rh-6 W-0.5 Hf-0.2 Ti	81,000	27.5
Pt-30 Rh-8 W-0.5 Hf-0.2 Ti	91,000	24.3
Pt-30 Rh-8 W-1 Hf-0.2 Ti	108,000	26.3
<u>1093°C (2000°F)</u>		
Pt-30 Rh	24,000	38
Pt-30 Rh-6 W	36,000	33.3
Pt-26 Rh-8 W	38,000	18
Pt-30 Rh-10 W	47,000	15.5
Pt-30 Rh-6 W-0.5 Hf-0.2 Ti	42,200	28.1
Pt-30 Rh-8 W-0.5 Hf-0.2 Ti	44,500	12.5
Pt-30 Rh-8 W-1 Hf-0.2 Ti	52,000	24.1

^aNot tested.

previously.¹ The hafnium and titanium improve the tensile strength of Pt-Rh-W base at all temperatures measured. This effect is more prominent at 1093°C. Table 4 shows that the 0.5% Hf-stabilized 8% W alloy is comparable to, and the 1% Hf alloy is stronger than, Pt-30% Rh-10% W. The room-temperature ductility of stabilized alloys is lower than that of the base. However, 1% Hf and 0.2% Ti improve the ductility of the Pt-30% Rh-8% W alloy from 18 to 24.1% at 1093°C.

The oxidation behavior of the Pt-26% Rh-8% W-1% Hf-0.2% Ti alloy in air has been determined. The alloy oxidized at an average rate of $+2 \times 10^{-7}$, -5×10^{-7} , and -6.7×10^{-6} g/cm².hr at 760, 1000, and 1200°C, respectively. Since the base ternary alloy Pt-26% Rh-8% W exhibits oxidation rates of $+2 \times 10^{-7}$, -1×10^{-6} , and $+6 \times 10^{-6}$ g/cm².hr, we conclude that the hafnium and titanium additions do not impair the excellent oxidation resistance of the ternary base.

Characterization of Iridium

Iridium metal is attractive in terms of its high melting point, desirable mechanical strength, and moderate oxidation resistance. However, the use of iridium as a cladding material for space isotopic heat sources is retarded because of many difficulties, such as low ductility, poor fabricability, and extremely large variations in mechanical properties. It is believed that the problems are caused by minor, as yet unidentified, impurities. The objective of this task is twofold: (1) to characterize the physical and mechanical properties of iridium, and (2) to resolve the major problems of ductility and fabricability.

Iridium metal in sheet and plate forms was purchased from Englehard Industries. To determine the recrystallization temperature, softening behavior, and bend ductility, 20-mil sheet in the warm-rolled condition was cut into strips and then annealed 1 hr in the 400 to 1600°C range. The microhardness data in Table 5 show a general decrease at low temperatures and a more

Table 5. Effect of 1-hr Annealing Treatment on Hardness, Recrystallization, and Bend Ductility of Unalloyed Iridium Sheet

Annealing Temp (°C)	Microhardness (DPH)	Recrystallization (%)	Results of 90° Bend Test at Room Temp
As received	490	0	Cracked
400	498	0	Cracked
600	478	0	Cracked
800	426	0	Cracked
1000	400	0	Microcracks
1100	365	0	Microcracks
1200	310	0	No cracks
1300	265	50	Microcracks
1400	221	100	Microcracks
1500	198	100	Cracked
1600	205	100	Cracked

rapid decrease above 1000°C. Metallographic examination reveals no indication of recrystallization at 1200°C, 50% recrystallization at 1300°C, and complete recrystallization at 1400°C. In the recrystallized condition, iridium has a hardness of about 200 DPH.

The effect of annealing treatment on the ductility was determined by bending strips 90° at room temperature and then examining them metallographically. All the annealed specimens show macro- and microcracks with the exception that no cracks were observed in the specimen annealed at 1200°C. All cracks were formed on grain boundaries, and their propagation caused the failure of specimens on bending.

Based on the bending data, the iridium sheet was ductilized by heat-treating 1 hr at 1200°C as tensile specimens were stamped out successfully at room temperature. Tensile tests at room and elevated temperatures are shown in Table 6. Iridium has quite low tensile strength at room temperature; however, its strength decreases slowly with increasing temperature. The strength data in Table 6 are in good agreement with the results for commercially pure iridium reported by Jaffee *et al.*² It should be noted that iridium is much weaker than the hafnium- and titanium-stabilized Pt-Rh-W alloys as shown in Table 4.

Table 6. Room- and Elevated-Temperature Tensile Properties of Unalloyed Iridium Recrystallized 1 hr at 1500°C

Testing Temperature (°C)	Ultimate Tensile Strength (ksi)	Elongation (%)
Room Temperature	56	5.7
760	56	23.5
1093	35	19.8

The ductility of iridium is low at room temperature and increases to 23.5% at 760°C. This result is also consistent with the work of Jaffee who found the ductile-to-brittle transition temperature of iridium to be ~600°C.

The recrystallized iridium sheet specimens were oxidized in static air at 1040, 900, and 770°C for 1100 hr. The results are described below:

Oxidation at 1040°C - No oxide layer is observed at this temperature. After 50-hr exposure, the material on the edge and surface of the specimen gradually loses its adhesion and begins to flake off in the form of metallic grains. However, the oxidation rate is quite linear at an average rate of -880×10^{-6} g/cm².hr. This value is in excellent agreement with the reported value (-900×10^{-6} g/cm².hr) by Jaffee *et al.*²

Oxidation at 900°C - An adherent dark blue oxide layer gradually appears on the surface of specimen at 900°C. The initial rate of oxidation is parabolic with a low oxidation rate. However, after 600-hr exposure,

the specimen begins to show corner effects and the oxidation rate increases to approximately -27×10^{-6} g/cm².hr.

Oxidation at 770°C - Although the dark blue oxide layer is observed to form, no apparent weight change can be measured at this temperature.

PHYSICAL METALLURGY OF REFRACTORY ALLOYS

(Division of Reactor Development and Technology Program 04 40 02 05 1)

R. G. Donnelly
Metals and Ceramics Division

The purpose of this program is to provide a base technology evaluation of high-temperature materials for use in space applications of radioisotope thermoelectric generators (RTG's). Emphasis is presently on tantalum and molybdenum alloys used as containment materials for ²³⁸PuO₂.

Effect of Oxygen Contamination on the Mechanical Properties of T-111

The tensile properties of 20-mil sheet specimens of T-111 oxygen-contaminated at 1000°C have been reported previously.³ In order to show the effects of specimen thickness and doping temperature, both 20- and 40-mil sheet specimens were doped with oxygen at 825°C and 1×10^{-5} torr oxygen pressure. The tensile properties of these specimens at temperatures up to 1093°C (2000°F) are presented in Tables 7 and 8. The tensile strength generally increases with amount of oxygen. The ductilities obtained at room and elevated temperatures are plotted, respectively, in Figs. 6 and 7 as a function of the amount of oxygen doped at 825 and 1000°C. The room-temperature ductility (Fig. 6) of T-111 doped at 1000°C decreases continuously with oxygen up to 700 ppm. Doping at 825°C causes only a moderate decrease of ductility at the lower oxygen levels (200 to 300 ppm) and a sharper decrease at higher levels. The ductility is sensitive to the specimen thickness; the 20-mil specimens can tolerate about 100 ppm more oxygen than 40-mil specimens. When tested at elevated temperatures (Fig. 7), the ductility keeps constant initially until a critical oxygen level is reached. The critical oxygen level varies with both the doping temperature and specimen thickness. Beyond that level, the ductility decreases continuously with oxygen content. For a strain of 5%, the T-111 can tolerate 480 and 560 ppm, respectively, for 40- and 20-mil specimens doped at 825°C, and 750 ppm at 1000°C. Tables 7 and 8 also indicate that at a given oxygen content, for example, 350 ppm in 40-mil specimens, the T-111 has higher ductility at 825°C (10%) than at room temperature (1.6%) or 1093°C (2.5%). Thus, there is no "ductile-to-brittle transition temperature" for oxygen-contaminated T-111; instead, there is a "ductility maximum" that fortuitously appears to occur near the heat source temperature of 825°C.

Table 7. Tensile Properties of 20-mil Sheet T-111
Specimens As-Doped with Various Levels of Oxygen at 825°C

Oxygen Added (ppm)	Elongation (%)	Ultimate Tensile Strength (psi)
<u>Room Temperature</u>		
0	28	101,000
302	19	111,000
400	2	100,000
641	1.3	125,000
770	0.8	150,000
<u>825°C</u>		
0	17.8	69,000
290	15	79,000
375	10.6	81,000
460	8.5	83,000
565	4.0	71,000
660	2.0	70,000
<u>1093°C</u>		
680	0.5	77,000

Table 8. Tensile Properties of 40-mil Sheet T-111
Specimens As-Doped with Various Levels of Oxygen at 825°C

Oxygen Added (ppm)	Elongation (%)	Ultimate Tensile Strength (psi)
<u>Room Temperature</u>		
162	25.5	99,500
215	20.5	106,000
300	1.6	96,000
391	0.5	114,000
<u>825°C</u>		
140	18	64,000
296	10.2	66,000
389	7.5	63,000
510	4.2	69,000
<u>1093°C</u>		
306	2.5	51,000
330	2.4	51,000

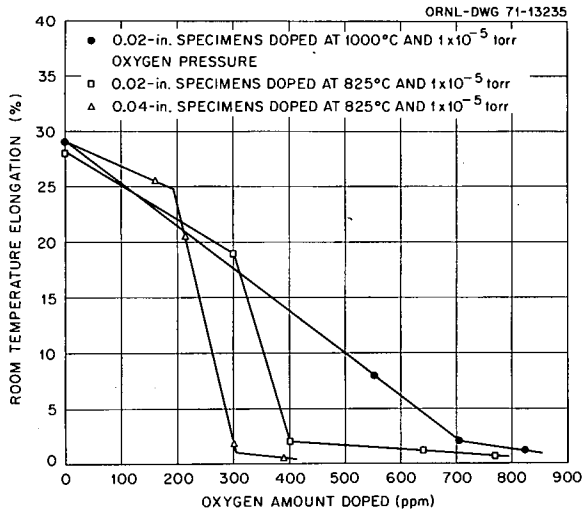


Fig. 6. Room-Temperature Ductility of T-111 Specimens as a Function of the Amount of Oxygen Doped at 825 and 1000°C.

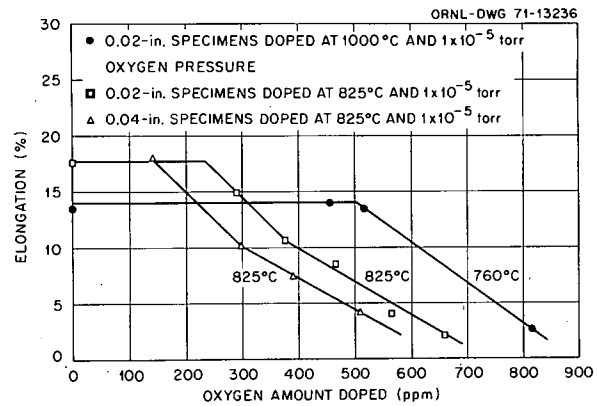


Fig. 7. Elevated-Temperature Ductility of T-111 Specimens as a Function of the Amount of Oxygen Doped at 825 and 1000°C.

The fracture process in the oxygen-contaminated specimens was examined during a room-temperature tensile test. The macroscopic cracks were observed to form first on the edges and surfaces which contain a higher level of oxygen and are therefore more brittle. The propagation of these cracks, once present, through the ductile core causes the low ductility of the specimens tested at room temperature and 1093°C. However, the edge and surface cracks do not propagate as easily when tested at 825°C; consequently, numerous cracks were observed on the fracture specimen as shown in Fig. 8B. In contrast, only a very few cracks were observed at room temperature and 1093°C (Fig. 8A and 8C).

The results so far indicate that both doping temperature and specimen thickness have a big effect on the properties of oxygen-contaminated T-111. It is also expected that the mechanical behavior of T-111 varies with the doping rate, because the doping rate affects the surface oxygen concentration and the oxygen gradient. It should be noted that the above data were obtained from specimens doped at a high rate (40 to 100 ppm/hr) and that different results may be obtained if different rates are used.

Effect of Oxygen on the Mechanical Properties of 0.090-in.-thick T-111

Previously, we reported that the oxygen concentration causing embrittlement of T-111 decreased as the doping temperature was decreased from 1000 to 825°C and also as the specimen thickness increased from 20 mils to 40 mils (see Figs. 6 and 7 in previous section). The doping rate of the above specimens at 825°C was also higher (80 ppm/hr for 20-mil and 40 ppm/hr for the 40-mil specimens) than that indicated in the Pioneer heat source. Because of these differences, a new series of specimens, 90 mils thick, is being doped with oxygen at a rate of 1.5 ppm/hr (1×10^{-6} torr O_2 at

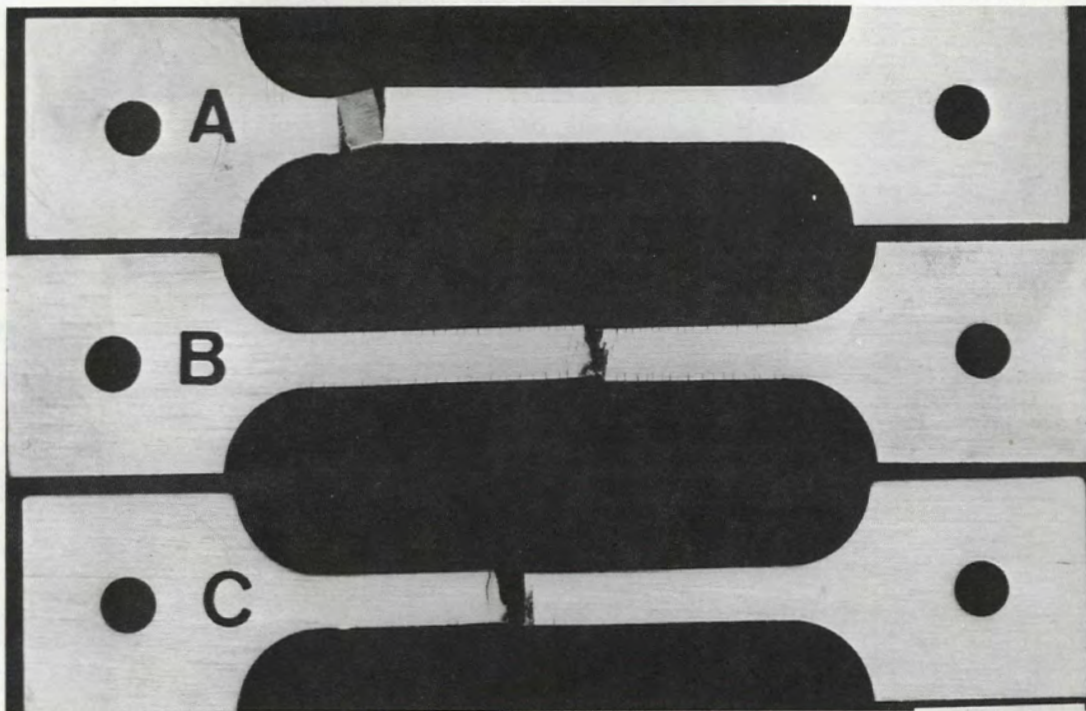


Fig. 8. Surface and Edge Cracking Behavior of T-111 Tensile Specimens Doped with Approximately 300 ppm Oxygen as a Function of Test Temperature. (A) Room Temperature, (B) 825°C, and (C) 1093°C.

825°C). In addition to these changes, the oxygen is being added to blanks 0.090 in. \times 3/4 in. \times 2-1/2 in. prior to machining the tensile specimens in order to eliminate oxygen from the edges of the specimen gage length which was present in the thinner specimens.

The tensile properties of the oxygen-doped, 90-mil-thick specimens, tested at 825°C are shown in Table 9. Up to 290 ppm O₂, the tensile strength increased with the oxygen content but did not impair the ductility at all. Figure 7 shows that the ductility is insensitive to the oxygen content at 825°C until a critical level is reached. Because this critical level decreased from approximately 240 ppm to 150 ppm O₂ as the specimen thickness increased from 20 to 40 mils, it was expected that the 90-mil specimens would have a still lower critical oxygen content. Therefore, these surprising results may be due to either a much lower oxygen doping rate and/or the elimination of oxygen from the edges of the tensile specimens by machining.

Table 9. Effect of Oxygen on the Tensile Properties of 90-mil-thick T-111 at 825°C

Oxygen Added (ppm)	Elongation (%)	Ultimate Tensile Strength (psi)
Control ^a	18.0	59,200
185	20.5	72,500
290	18.5	77,500

^aAnnealed 1 hr at 1650°C. Annealed analysis: 10 ppm oxygen, 10 ppm nitrogen, 3 ppm hydrogen, and 24 ppm carbon.

Contamination Studies of T-111 and TZM by Impurities Outgassed from Graphite and Min-K 1301

Tensile specimens of bare T-111, molybdenum-coated T-111, and TZM are being exposed at 825°C to an environment that approximates that in the Pioneer heat source. The environment consists of about 600 torr argon plus the impurity gases outgassed from a 70-g cylinder of ATJ graphite and 1.6 g of Min-K 1301, both at 538°C.* Both bare and palladium-wrapped zirconium sheet 0.010 × 0.5 × 0.6 in. long was wrapped around the graphite cylinder to getter the impurities. Copper oxide at 190°C was used as a stand-in for PuO₂.

The chemistry changes and the reaction rates of T-111 based on the weight gain of the specimens are shown in Table 10. These results show that the average contamination rate is constant (i.e., weight gain varies linearly with time). The scatter among the duplicate and triplicate specimens is attributed to the shielding of the active gases by the adjacent specimens. Specimen T-12 scheduled for a 1000-hr exposure was terminated at 534 hr when the specimen fractured during handling.

The contamination rate of T-111 by the gases outgassed from graphite but gettered with zirconium (without argon cover gas and Min-K) was 6400 ppm in 200 hr or 32 ppm/hr. Table 10 shows that the rate in the simulated Pioneer environment averaged 11.4 ppm/hr. Thus, it appears that 600 torr of argon lowers the reaction kinetics by about a factor of 3.

Molybdenum coatings continue to show their effectiveness in lowering the contamination of T-111. As shown in Table 10, 0.1 mil of evaporated molybdenum lowers the contamination rate of T-111 by a factor of about 3, 0.2 mil lowers the rate by a factor of about 6, and a coating thickness of 1.2 mils completely protected T-111 for 496 hr. The edges of the T-111 specimen coated with 0.2 mil of evaporated molybdenum fragmented into a black powder and consumed about one-half of the tensile specimen after 1030 hr of exposure. This specimen was unsuitable for tensile testing.

*ATJ graphite was vacuum outgassed 4 hr at 1200°C. The Min-K was baked in air 48 hr at 400°C. Both were then vacuum outgassed in the contaminating apparatus for 2 hr at 600°C to a pressure of 10⁻⁶ torr.

Table 10. Contamination of 0.020-in.-thick Sheet Specimens of T-111 and Molybdenum-Coated T-111 in a Simulated Pioneer Heat Source Environment

Material	Sample Number	Exposure (hr)	Calcd ^a Contamination (ppm)	Rate (ppm/hr)
T-111	T-10	204	1900	9.3
	T-11	204	2040	10.0
	T-12	204	3290	16.1
	Average			11.8
T-111	T-11	534	5400	10.1
	T-12	534	6480	12.1
	Average			11.1
0.1-mil Mo on T-111	T-M-3	204	820	4.0
0.2-mil Mo on T-111	T-M-4	204	460	2.2
		534	800	1.5
	Average			1.8
1.2-mil Mo on T-111	T-MC-2	496	0 ^b	0

^aBased on weight gain of specimens.

^bSpecimen lost weight.

The coating on the T-111 specimen coated with 0.2 mil of evaporated molybdenum plus 1.0 mil of CVD molybdenum failed after 802 hr of exposure at coating defects in the specimen shoulders in the manner described above. The intact gage section of this specimen was bent without failure through a 1T bend at room temperature. From this result, the ductility in the outer fiber of the 20-mil specimen was estimated to be approximately 30% and the oxygen contamination <100 ppm (see Table 11). The contamination of TZM could not be calculated since the specimens lost about 0.0001 g (out of 2.3 g) in 1030 hr. The room-temperature tensile tests conducted to date are summarized in Table 11. Bare T-111 shows complete embrittlement as would be expected for specimens containing several thousand parts per million of oxygen.

Table 11. The Effect of Impurities Degassed from Graphite and Min-K 1301 on the Room Temperature Tensile Properties^a of 20-mil-thick T-111 and TZM

Material	Exposure (hr)	Oxygen Contamination (calcd ppm)	Ultimate Tensile Strength (psi)	Elongation (%)
T-111	204	1900	113,000	0 ^b
T-111	534	6480	Fractured on handling	
0.1 mil Mo on T-111	204	820	139,000	
0.2 mil Mo on T-111	1030	—	Fragmented in environment	
1.2 mil Mo on T-111	802	<100 (est)	—	~30 ^c
TZM	534	Not determined	77,800	35.7
TZM	1030	Not determined	78,400	32.8
TZM	Control	—	79,600	33.5

^aSpecimen at 825°C; graphite and Min-K at 538°C; environment of 600 torr argon plus impurities.

^bFractured in shoulder of specimen.

^cEstimated, based on bend test.

The results for TZM clearly show that the simulated Pioneer environment has no effect for exposures to 1030 hr at 825°C. Exposures to 2000 hr for additional TZM specimens have been completed and are being evaluated.

Contamination Studies of T-111 and TZM by Water Vapor

Since water vapor is a probable contaminant in Pioneer generators, the effect of exposures of T-111 and TZM to this environment is being evaluated. The chemistry change of T-111 calculated from the weight gain of tensile specimens after several exposure times to 1×10^{-5} torr water vapor are tabulated in Table 12. These data show that the contamination rate up to 676 ppm is constant but decreases with the exposure time as the contamination level increases further. Based on prior work, the weight gain in water vapor is due only to oxygen contamination.⁴ Visual evidence of a reaction was not detected in either T-111 or TZM. Exposures of 20-mil TZM specimens (approximate weight = 2.4 g) to 1×10^{-5} torr water vapor at 825°C show an average weight loss of 0.0005 g after 457 hr. At 1002 hr of exposure, a very small weight increase of 0.000032 g was measured.

Table 12. Contamination of T-111 Exposed to 1×10^{-5} Torr Water Vapor at 825°C

Specimen Thickness (in.)	Exposure (hr)	Calculated ^a Contamination (ppm)	Rate (ppm/hr)
0.020	16	308 ^b	19.2
	32	676 ^b	21.1
	216	2735 ^c	12.7
	457	4155 ^c	9.1
0.040	16	196 ^c	12.2
	32	410 ^c	12.8

^aBased on weight gain of specimens.

^bAverage of 4.

^cAverage of 2.

The effect of water vapor contamination on the tensile properties of T-111 are listed in Table 13. These results show that the ductility is seriously impaired at about the same levels indicated in oxygen contamination tests.

Table 14 shows the tensile properties of TZM after exposure to water vapor. The room-temperature tests show a small decrease in the elongation that appears to become more serious with the exposure time. The tensile strengths of the exposed specimens are also higher than the control. Although the tests at 825°C show evidence of some loss of ductility, elongation of approximately 16% is characteristic of recrystallized and uncontaminated TZM at 982°C.⁵ Exposures of TZM to 2000 hr have been completed and are being evaluated.

Table 13. Effect of Water Vapor Contamination on the Room-Temperature Tensile Properties of T-111

Oxygen Contamination Level ^a (ppm)	Specimen Thickness (in.)	Tensile Strength (ksi)	Elongation (%)
Control	0.020	101	28
311	0.020	109	12.3
720	0.020	135	0.8
187	0.040	102	27.5
395	0.040	107	4.0

^aCalculated from weight gain of specimen.

Table 14. Tensile Properties of 20-mil-thick TZM Exposed to 1×10^{-5} Torr Water Vapor at 825°C

Test Temperature (°C)	Exposure (hr)	Ultimate Tensile Strength (psi)	Elongation (%)
Room	Control	79,600	33.5
Room	457	83,200	31.0
Room	1002	80,600	29.3
825	Control	45,000	24.8
825	457	45,600	20.2
825	1002	46,000	16.3

Effect of Oxygen Contamination on the Mechanical Properties of Molybdenum-Base Alloys

In order to qualify the use of molybdenum-base alloys as the cladding material for space isotopic heat sources, 20-mil TZM and Mo-46% Re sheet specimens were doped with oxygen at 825 and 1000°C and at 1 to 4×10^{-5} torr oxygen pressure. TZM shows a weight loss due to evaporation of molybdenum oxide, and molybdenum-rhenium alloy shows a small weight gain under low-oxygen pressure. For example, TZM loses 3800 ppm after 2000-hr exposure and molybdenum-rhenium gains 800 ppm after 1000-hr exposure at 825°C.

The contaminated specimens were then tested in tension at various temperatures; the results are presented in Tables 15 and 16. The data in Table 15 indicate that oxygen contamination of TZM at 825°C only causes a small increase of tensile strength and a moderate decrease of ductility. As a

Table 15. Tensile Properties of 20-mil-thick TZM and Mo-46% Re Sheet Specimens Contaminated with Oxygen at 825°C

Alloy	Doping Condition		Elongation (%)	Ultimate Tensile Strength (psi)
	Time (hr)	Oxygen Pressure (torr)		
<u>Room Temperature</u>				
TZM	a	a	37	79,000
	a	a	33.5	79,600
	110	4×10^{-5}	35.3	81,200
	500	1×10^{-5}	29.2	85,000
	2000	1×10^{-5}	24.5	85,000
Mo-46% Re	a	a	8.2	195,000
	1000	1×10^{-5}	9.2	192,000
<u>825°C</u>				
TZM	a	a	24.8	45,000
	2000	1×10^{-5}	17.7	51,200
Mo-46% Re	1000	1×10^{-5}	13.7	116,000

^aAs recrystallized.

matter of fact, TZM has 24.5% strain at room temperature and 17.7% at 825°C after 2000-hr exposure. No apparent change of mechanical properties of Mo-46% Re is observed after 1000-hr exposure. All these results indicate that the molybdenum-base alloys are compatible with low-pressure oxygen at 825°C.

Table 16 shows the effects of testing temperature and heat treatment on the tensile properties of TZM specimens doped at 1000°C and 1×10^{-5} torr oxygen pressure. The as-doped specimen was extremely brittle and fractured within the elastic limit when tested at room temperature. Increasing the test temperature to 1093°C does not improve the ductility significantly. But the ductility of the specimen is completely restored after 15 min heating at 1700°C. These results clearly indicate that TZM and T-111 behave similarly after oxygen contamination.⁶ However, due to the low rate of oxygen penetration in molybdenum matrix, it is important to note that, from the standpoint of environmental stability, TZM may be suitable as a cladding material for space power systems when the operation temperature is low, for example, 825°C, as in the Pioneer radio-isotope thermoelectric generators.

Effect of CO-Gas Contamination on the Mechanical Properties of Molybdenum-Base Alloys

The 20-mil sheet specimens of TZM and Mo-46% Re alloys were contaminated at a CO pressure of 1×10^{-5} torr and 825°C. The amount of contamination is controlled by doping time. Both alloys show a small weight gain after

Table 16. Effects of Heat Treatment and Testing Temperature on the Tensile Properties of TZM Specimens Doped with Oxygen for 207 hr at 1000°C and 1×10^{-5} Torr Oxygen Pressure

Heat Treatment	Testing Temperature (°C)	Elongation (%)	Tensile Strength (psi)
None	Room Temperature	0 ^a	5000-7000
None	825	2.5	63,000
None	1093	0.7	48,100
15 min at 1700°C	Room Temperature	31.6	85,000

^aFracture within the elastic limits.

long-time exposure. The contaminated specimens were then tested in tension at room temperature and 825°C; the data are presented in Table 17. Both the tensile strength and elongation of the contaminated specimens are not significantly different from the as-recrystallized ones, even after 2000-hr exposure. We, therefore, conclude that the molybdenum-base alloys are compatible with CO gas at 825°C. These results combined with the results of oxygen contamination and exposure to graphite and Min-K reported in the previous sections lead to the general conclusion that, from the standpoint of environmental stability, TZM and Mo-46% Re alloys are suitable for use as fuel cladding materials for Pioneer space power systems whose operation temperature is in the range of 800 to 850°C.

Table 17. Tensile Properties of 20-mil-thick TZM and Mo-46% Re Sheet Specimens Contaminated with CO Gas at 825°C and 1×10^{-5} Torr Oxygen Pressure

Alloy	Doping Time (hr)	Elongation (%)	Tensile Strength (psi)
<u>Room Temperature</u>			
TZM	0	37.0	79,000
	0	33.5	79,600
	196	33.2	79,500
	1000	30.0	83,000
	2000	27.9	82,000
Mo-46% Re	0	8.2	195,000
	1004	10.7	190,000
<u>825°C</u>			
TZM	0	24.8	45,000
	2000	22.5	46,300
Mo-46% Re	1004	10.5	115,000

MATERIALS COMPATIBILITY TESTING FOR THE LASL-DART PROJECT

*J. R. DiStefano and A. C. Schaffhauser
Metals and Ceramics Division*

We are testing several nonfuel materials that may be used in constructing the DART (Decomposed Ammonia Radioisotope Thruster) for Los Alamos Scientific Laboratory.

Compatibility couples of graphite with several materials were heated for 500 hr at 1300, 1400, and 1500°C, and the results are given in Table 18. On the basis of our visual observations, tungsten showed the least interaction with graphite. The molybdenum sample was embrittled and crumbled after exposure at 1500°C. Samples for metallographic and chemical analyses have been submitted.

Additional 500-hr tests of several materials in metallic capsules have been completed. Test conditions are listed in Table 19.

Table 18. Visual Observations from Compatibility Tests of Graphite With Several Materials for 500 hr at 1300, 1400, and 1500°C

Specimen	Visual Observations		
	1300°C	1400°C	1500°C
Tantalum	R, S	R, S	R, S, D
Tungsten	NR	NR	SR
Molybdenum	R	R, D, S	R, ^a D, S
Rhenium	S	S	S
Mo-50% Re	S, D	R, S, D	S, D
Pt-Rh-W	R, S, D	R, S, D	R, S, D
BeO	D	D	R, D

R = Visible reaction between graphite and specimen.

S = Specimen stuck to graphite.

NR = No visible reaction.

SR = Slight reaction.

D = Surface of specimen discolored.

^aSpecimen crumbled.

Table 19. Conditions for 500-hr Metal Capsule Compatibility Tests

Specimen Materials		Temperature (°C)	Test Atmosphere
Capsule	Test		
Molybdenum	ZrO ₂ , HfO ₂ , BeO	1300, 1400, 1500	DV
Molybdenum	BeO	1300, 1400, 1500	SV
Tungsten	ZrO ₂ , HfO ₂ , BeO	1300, 1400, 1500	DV
Tungsten	BeO	1300, 1400, 1500	SV
Tantalum	ZrO ₂ , HfO ₂	1300, 1400, 1500	DV
Rhenium	BeO	1400, 1500	DV
Mo-50% Re	BeO	1400, 1500	DV
Molybdenum	Rhenium	1300, 1400, 1500	DV
Tungsten	Rhenium	1300, 1400, 1500	DV
Tungsten	Mo-50% Re	1300, 1400, 1500	DV
Mo-50% Re	Iridium	1400, 1500	DV

DV = Dynamic vacuum. SV = Static vacuum.

REFERENCES

1. Eugene Lamb, *ORNL Isotopic Power Fuels Quarterly Report for Period Ending September 30, 1971*, ORNL-4750, Oak Ridge National Laboratory.
2. R. I. Jaffee *et al.*, "Re and the Refractory Pt-Group Metals," p. 383 in *Refractory Metals and Alloys*, Vol II, M. Semchyshen and J. J. Harwood (eds.), Interscience, New York, 1961.
3. Eugene Lamb, *ORNL Isotopic Power Fuels Quarterly Report for Period Ending March 31, 1971*, ORNL-4692, Oak Ridge National Laboratory.
4. M. D. Ketchum and C. A. Barrett, *Contamination of Refractory Metals by Oxygen, Water Vapor, and Carbon Monoxide*, NASA-CR-1537 (May 1970).
5. M. Semchyshen and R. Q. Barr, *Symposium on Newer Metals*, Special Technical Publication No. 272, ASTM (1959), pp. 1-24.
6. Eugene Lamb, *ORNL Isotopic Power Fuels Quarterly Report for Period Ending June 30, 1971*, ORNL-4723, Oak Ridge National Laboratory.

ORNL-4774
UC-33 - Propulsion Systems and
Energy Conversion

INTERNAL DISTRIBUTION

- | | |
|--|-----------------------------------|
| 1-3. Central Research Library | 39. E. Lamb |
| 4. ORNL - Y-12 Technical Library
Document Reference Section | 40. R. E. Leuze |
| 5-24. Laboratory Records Department | 41. H. G. MacPherson |
| 25. Laboratory Records, ORNL R.C. | 42. R. E. McHenry |
| 26. G. M. Adamson, Jr. | 43. A. J. Miller |
| 27. P. S. Baker | 44. S. J. Rimshaw |
| 28. T. A. Butler | 45-46. R. A. Robinson |
| 29. W. R. Casto | 47. A. F. Rupp |
| 30. F. L. Culler | 48. R. W. Schaich |
| 31. J. E. Cunningham | 49. M. J. Skinner |
| 32. R. G. Donnelly | 50. A. H. Snell |
| 33. D. E. Ferguson | 51. D. A. Sundberg |
| 34. J. H. Frye, Jr. | 52. D. B. Trauger |
| 35. R. F. Hibbs | 53. A. M. Weinberg |
| 36. M. R. Hill | 54. C. M. Adams, Jr. (consultant) |
| 37. H. Inouye | 55. Walter Kohn (consultant) |
| 38. Lynda Kern | 56. Sidney Siegel (consultant) |

EXTERNAL DISTRIBUTION

57. R. D. Baker, Los Alamos Scientific Laboratory, Los Alamos, N.M.
58. R. T. Carpenter, Division of Space Nuclear Systems, AEC, Washington
59. Commander, Naval Undersea Research and Development Center, San Diego, California 92132, Attn: Technical Library, Code 133
60. C. R. Crane, Headquarters AFSC (XRTS), Andrews Air Force Base, Maryland 20331
61. G. P. Dix, Division of Space Nuclear Systems, AEC, Washington
- 62-64. E. E. Fowler, Director, Division of Applied Technology, AEC, Washington
65. D. S. Gabriel, Director, Division of Space Nuclear Systems, AEC, Washington
66. W. B. Creamer, Area Manager, Dayton Area Office, AEC, Miamisburg, Ohio
67. G. L. Hagey, Naval Fac. Engr. Command, Nuclear Power Division, Washington
68. R. C. Hamilton, IDA - Rm 19, 400 Army-Navy Drive, Arlington, Va.
69. R. E. Hopkins, U.S. Army Mobility Equipment R and D. Center, Ft. Belvoir, Va.
70. T. B. Kerr, Code RY, NASA Headquarters, Washington
71. F. E. Kruesi, Director, Savannah River Laboratory, Aiken, S.C.
72. J. A. Lieberman, Division of Reactor Development and Technology, AEC, Washington
73. W. A. McDonald, Isotopes, Inc., Nuclear Systems Division, 110 West Timonium Road, Timonium, Maryland 21093
74. R. L. Neubert, Vice President and Director, Mound Laboratory, Miamisburg, Ohio, Attn: W. T. Cave

75. G. A. Newby, Division of Space Nuclear Systems, AEC, Washington
76. J. A. Powers, Division of Space Nuclear Systems, AEC, Washington
77. A. A. Pitrolo, Manager, MHW-RTG Program, Isotope Power Systems Operation, General Electric Company, Space Division, P.O. Box 8661, Philadelphia, Pennsylvania
78. F. C. Schwenk, Division of Space Nuclear Systems, AEC, Washington
79. S. J. Seiken, Division of Reactor Development and Technology, AEC, Washington
80. M. Shaw, Director, Division of Reactor Development and Technology, AEC, Washington
81. J. A. Swartout, Union Carbide Corporation, New York, N.Y.
82. D. G. Williams, Manager, AEC, Richland Operations Office, Richland, Washington
83. Director, Pacific Northwest Laboratory, Richland, Washington
84. AEC, Savannah River Operations Office
85. General Electric Company, MSD, AEC
86. General Electric Company, VNC, AEC
87. Isotopes, Inc., Middle River, AEC
88. NASA, Goddard Space Flight Center
89. NASA, Langley Research Center
90. NASA, Manned Spacecraft Center
91. NASA, Marshall Space Flight Center
92. Navy Space Systems Activity
93. Radio Corporation of America, AEC
94. Sanders Nuclear Corporation, AEC
95. Thermo Electron Corporation, AEC
96. Laboratory and University Division, AEC, ORO
97. Patent Office, AEC, ORO
- 98-271. Given distribution as shown in TID-4500 (59th ed.) under Propulsion Systems and Energy Conversion category (25 copies - NTIS)